Wear, Vol. 382-383, 15 July 2017, pp. 78-84
DOI:10.1016/j.wear.2017.04.013

Author's Accepted Manuscript

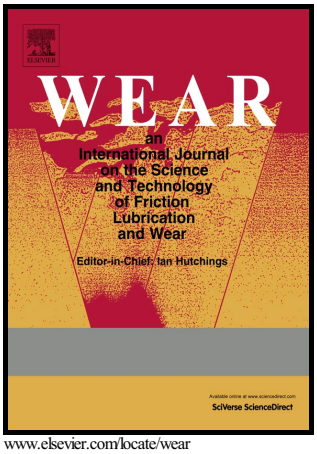

www.elsevier.com/locate/wear

Reciprocating sliding wear behavior of high-strength nanocrystalline $Al_{84}Ni_7Gd_6Co_3$ alloys

Z. Wang, K. Georgarakis, W.W. Zhang, K.G. Prashanth, J. Eckert, S. Scudino

PII: S0043-1648(16)30799-2
DOI: http://dx.doi.org/10.1016/j.wear.2017.04.013
Reference: WEA102142

To appear in: *Wear*

Received date: 16 December 2016
Revised date: 29 March 2017
Accepted date: 21 April 2017

Cite this article as: Z. Wang, K. Georgarakis, W.W. Zhang, K.G. Prashanth, J. Eckert and S. Scudino, Reciprocating sliding wear behavior of high-strengt nanocrystalline $Al_{84}Ni_7Gd_6Co_3$ alloys, *Wear* http://dx.doi.org/10.1016/j.wear.2017.04.013

Reciprocating sliding wear behavior of high-strength nanocrystalline $Al_{84}Ni_7Gd_6Co_3$ alloys

Z. Wang [a*], K. Georgarakis [b], W.W. Zhang [a], K.G. Prashanth [c,d], J. Eckert [c,e], S. Scudino [f]

[a]School of Mechanical and Automotive Engineering, South China University of Technology, Guangzhou 510640, China

[b]School of Aerospace, Transport and Manufacturing, Cranfield University, MK430AL Cranfield, United Kingdom

[c]Erich Schmid Institute of Materials Science, Austrian Academy of Sciences, Jahnstraße 12, A-8700, Leoben, Austria

[d]Department of Manufacturing and Civil Engineering, Norwegian University of Science and Technology, Teknologivegen 22, 2815,Gjovik, Norway

[e]Department Materials Physics, Montanuniversität Leoben, Jahnstraße 12, A-8700 Leoben, Austria

[f]Solidification Processes and Complex Structures, Institute for Complex Materials, IFW Dresden, Helmholtzstraße 20, D-01069 Dresden, Germany

[*]Corresponding author: Dr. Z Wang, School of Mechanical and Automotive Engineering, South China University of Technology, Guangzhou 510640, China. wangzhi@scut.edu.cn

Abstract

Nanocrystalline Al-Ni-Gd-Co alloys with exceptionally high hardness have been recently developed from amorphous precursors. In the present work, the reciprocating sliding wear in the gross slip regime of these novel nanocrystalline Al-based alloys has been investigated under small amplitude oscillatory sliding motion using a martensitic chrome steel as the counter material. When compared to pure Al or Al-12Si alloy, these nanocrystalline alloys exhibit excellent wear resistance and a lower coefficient of friction when sliding against steel. The

enhanced wear resistance of the novel nanocrystaline Al alloys is related to their ultra-high hardness and the hybrid nanostructure that mainly consists of nanometric intermetallic phases embedded in a nanocrystalline fcc-Al matrix. Three body abrasive conditions were created at the initial stages of the wear tests due to the formation of micro- and nano-particulate debris from the worn surface of the Al alloys; the debris was compacted under the subsequent sliding cycles forming layers that are protective to the extensive wear of the Al alloys.

Keywords: Wear; Nanocrystalline alloys; Al alloys; Reciprocating sliding wear; Fretting wear; Tribological behavior

1. Introduction

Nanocrystalline (NC) and ultrafine grained (UFG) Al-based alloys have been the subject of intensive research over the last decades owing to their high room temperature strength combined with low density [1, 2]. A variety of high-strength Al-based alloys have been produced as large-scale bulk samples by consolidation and crystallization of glassy powders; although high tensile strength has been obtained in a few cases, most often consolidated Al alloys only show high compressive strength [2]. Compared to conventional coarse-grained Al alloys, the mechanical strength of which usually does not exceed 700 MPa, nanocrystalline Al-based alloys obtained from metallic glass precursors poses mechanical strengths that often reach values as high as 1 GPa [3, 4]. Recently, a novel $Al_{84}Ni_7Gd_6Co_3$ alloy with hybrid nanostructure and super-high mechanical strength up to ~1.8 GPa in compression has been developed [5], which is the highest strength ever reported for bulk Al-based alloys. The combination of exceptionally high strength and low density (~3.75 g cm^{-3}) leads to excellent specific engineering properties, such as specific strength of 496 kNm kg^{-1} and specific Young's modulus of 32 MNm kg^{-1}. The discovery of this

super-high strength $Al_{84}Ni_7Gd_6Co_3$ alloy is highly promising for the development of a new generation of high-strength Al alloys for advanced structural applications.

Despite the high potential of nanocrystalline Al-based alloys for engineering applications, research has mainly focused on processing, microstructural and mechanical properties investigations [6-11], whereas friction and wear behavior have attracted negligible attention so far. However, for many engineering applications (including in automotive applications like pistons and cylinder heads) wear accounts for more than 50% of materials losses in service [12-14] and thus the exploration of the tribological properties and wear resistance of the novel nanocrystalline Al alloys is of critical importance.

The wear behavior of many engineering components is often determined by the nature and micro-structure of surface films and coatings deposited by various methods, including electrodeposition, spray and sputtering techniques [15-18]. Among the aluminum based alloys, aluminum-silicon alloys exhibit good resistance against the fretting cracking [19-21]. The wear resistance of nanostructured materials (either in coatings or bulk form) is usually superior to that of their coarser-structured counterparts, which can be mainly attributed to their higher hardness following the well-known Hall-Petch relation down to average grain sizes of about 10 nm. For nanostructured materials with grain sizes below a critical value that is often of the order of 10 nm, hardness decreases as the decrease of the grain size, entering the so called "inverse Hall-Petch rregime" [1, 18, 22-23]. High wear resistance has been shown for the case of Al-based nanostructured alloys produced by rapid quenching techniques in the form of thin foils and ribbons [24]. However, the tribological properties of bulk nanostructured Al alloys have not been adequately addressed. In this work, the wear behavior of the super-high strength bulk $Al_{84}Ni_7Gd_6Co_3$ alloy is studied under small amplitude oscillatory relative motion against a

martensitic chrome steel counter-face using a fretting wear apparatus. The friction coefficient, wear resistance and wear mechanisms have been investigated and compared with the behavior of pure Al and Al-Si under similar conditions.

2. Experimental methods

$Al_{84}Ni_7Gd_6Co_3$ (at.%) bulk cylinders were produced by hot pressing of gas-atomized powders; two processing routes were examined in the present study: a) alloys produced by hot pressing of gas-atomized (as-atomized) powders (HP0) and b) alloys produced by hot pressing of gas-atomized and ball-milled for 100 h powders (HP100). Approximately 3.5 g of powder was first placed in a die of 10 mm diameter and hot pressed in a chamber under vacuum using the following parameters: pressure of 640 MPa, temperature of 773 K and dwell time of 3 min. Cylindrical specimens with 10 mm diameter and 15 mm length were used for the reciprocating sliding wear experiments. Three independent trials were conducted for each condition. For comparison, pure Al specimens were produced by hot–pressing using the same parameters. Furthermore, the wear behavior of the nanocrystalline Al alloys was compared with that of a cast Al-12Si (wt%) alloy, previously reported to exhibit good wear resistance due to its eutectic microstructure [25-27]. The cylindrical specimens were polished using SiC paper from 400 down to 4000 grit and subsequently polished using 3 μm and 0.25 μm diamond suspensions. Reciprocating sliding wear experiments were performed using an OPTIMOL SRV device (Munich, Bavaria, Germany) under unidirectional sliding conditions according to the ASTM-D5707-97 standard. The samples were tested against a steel ball (G-Cr 15) with a diameter of 10 mm. A preload of 5 N for 30 s was initially applied over the sample and steel ball. The wear tests were conducted at a load of 10 N for 30 min with a frequency of 50 Hz and half-slip amplitudes

in the range of 0.1 to 1 mm at ambient temperature and humility of ~50%. A computerized system was used to record the test parameters such as frequency, load, duration, friction coefficient, speed and temperature. The wear tracks were characterized by scanning electron microscopy (SEM) using a JEOL microscope. The three-dimensional topography of each wear scar was characterized by the BMT Expert3D morphology analyzer with a lateral resolution of 1 μm and the highest vertical resolution approaching 1 nm.

3. Results and discussion

3.1. Microstructure

The hot pressing of the $Al_{84}Ni_7Gd_6Co_3$ as-atomized (HP0) and ball milled (HP100) amorphous powders resulted in high densification of the nanocrystalline alloys producing bulk specimens with density of ~3.75 g/cm^3 and low porosity (less than 0.5 vol.%). The microstructure of the hot pressed bulk $Al_{84}Ni_7Gd_6Co_3$ alloys is shown in Fig. 1 (for additional details see Ref. [5]). The HP0 specimen, Fig. 1a, mainly consists of regions with relatively coarse precipitates with a high volume fraction of nanometric intermetallic phases distributed in the fcc-Al matrix. The HP100 specimen exhibits a bimodal-like microstructure consisting of the regions with coarse and fine precipitates. The difference between the two microstructures is a result of the high-energy ball milling process applied only to the HP100 specimen prior to consolidation. Both regions with coarse and fine precipitates exhibit hybrid structures consisting of nanometric intermetallic phases and nanocrystalline fcc-Al matrix. The nanometric intermetallic phases are identified as $Al_{19}Gd_3Ni_5$ intermetallic compounds (nanometric rod-like), Al_3Gd and Al_9Co_2 (equiaxed particle-like) [5]. The size of the intermetallic phases ranges between tens to hundreds of nanometers, while the grain size of fcc-Al is of the order of 100 nm

[5]. The volume fraction of the intermetallic phases is as high as ~80 vol.%. Owing to the high volume fraction of the hard intermetallic phases (nanohardness: 6-9 GPa) and the confinement effect between the phases, HP0 and HP100 samples exhibit super-high strength and hardness [5]. More specifically, the Vickers hardness increases from ~3.1 GPa for HP0 to ~4.3 GPa for HP100, whereas the mechanical strength in compression was found to be ~1.4 GPa for HP0 and ~1.8 GPa for HP100 [5]. For comparison, the Vickers hardness of pure Al (average grain size: ~10 μm) and Al-12Si alloy (average grain size: ~22 μm) are ~0.3 GPa and ~0.6 GPa, respectively, whereas the yield strength of pure Al is about ~63 MPa and ~104 MPa for Al-12Si [27,28]. Further analysis on the synthesis process and microstructural characterization of the $Al_{84}Ni_7Gd_6Co_3$ was recently reported in Ref. [5].

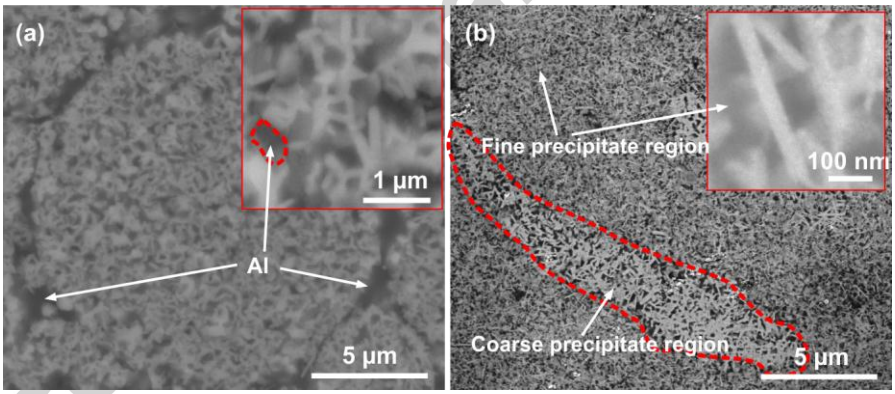

Fig. 1. SEM micrographs of $Al_{84}Ni_7Gd_6Co_3$ alloys: a) microstructure of HP0 specimens (consolidated gas-atomized powders), and b) microstructure of HP100 specimens (consolidated ball-milled powders).

3.2. Reciprocating sliding wear tests

The reciprocating sliding wear behavior of the nanocrystalline $Al_{84}Ni_7Gd_6Co_3$ alloys was studied under small amplitude oscillatory motion, for half-amplitudes in the range of 0.1 to 1 mm, relative to a martensitic chrome steel counter-face. Fig. 2a shows the kinetic friction

coefficient (f_k) between the counter-surfaces as a function of the sliding cycles at half - amplitude of 1 mm. The friction coefficient during oscillatory sliding motion was shown to be independent from the sliding amplitude for sliding amplitudes higher than 50 μm [29]. HP0 and HP100 specimens exhibit similar trends with the friction coefficient between the counter-surfaces decreasing rapidly to a minimum value of about 0.38 after the initial running-in stage at approximately 5000 cycles, probably due to the formation and lubricating action of an oxide film that forms on the surface of Al-based materials and the removal of the initial roughness during the running-in period, which may result in a drop of the contact pressure. The rapid decrease of the friction coefficient is then followed by a gradual increase until it reaches a steady-state regime after about 35000 cycles, where the friction coefficient fluctuates around a mean value of about 0.7. This behavior could be attributed to the breakdown of the oxide film and the increase of adhesive frictional forces due to an increase of direct metal-to-metal contact areas [29]. In addition the formation of a higher density of debris particles in the contact between the counter-surfaces can also contribute to the observed increase of the friction coefficient, as well as to the fluctuation of the recorded friction coefficient values as seen in figure 2a. Fig 2b compares the mean friction coefficient between the counter-surfaces at the steady-state regime for the $Al_{84}Ni_7Gd_6Co_3$ super-hard alloys (HP0 and HP100) with those obtained for pure Al and Al-12Si. The friction coefficient for HP0 and HP100 (f_κ~0.7) appears to be noticeably lower than that for pure Al (f_κ~1.1) and Al-12Si (f_κ~1). The friction coefficient between two materials in relative motion depends on various parameters including the chemistry and surface properties of the counter-surfaces and the conditions of the relative motion [16, 30]. In the present case of Al-based alloys, the lower friction coefficient of the nanocrystalline $Al_{84}Ni_7Gd_6Co_3$ alloys could be mainly attributed to the surface phenomena occurring in the tribo-systems during the relative

sliding motion of the counter-surfaces. The surface phenomena include the formation of surface oxide layers as well as the formation of a tribo-layer of debris between the contact surfaces, while the exact nature (chemistry and crystal structure) of the surface oxides forming in this tribosystem has not been identified in this work. The high hardness of the $Al_{84}Ni_7Gd_6Co_3$ surfaces, (about 5 to 10 times higher than that of pure Al and Al-12Si), plays an important role for achieving lower levels of local plastic deformation at the asperities in contact with the counter surface and impede the disruption of the surface oxide film, thus hindering the direct metal-to-metal contact points between the two counter-surfaces [30-32]. Instead of the direct disruption of the surface oxide film by the counter material, a mild abrasion along with an oxidative wear mechanism may be the dominant mechanism for the $Al_{84}Ni_7Gd_6Co_3$ super-hard alloys. On the other hand, on the softer surfaces the local pressure on asperities can more easily lead to plastic deformation and breakdown of the surface oxide layers increasing the level of direct metal-to-metal contact between the tribo-materials, thus giving a rise to adhesive frictional forces. In addition, the more extensive local plastic deformation on the softer surfaces may potentially cause higher temperature rise on the surface that may also lead to more intensive adhesion between the counter-surfaces.

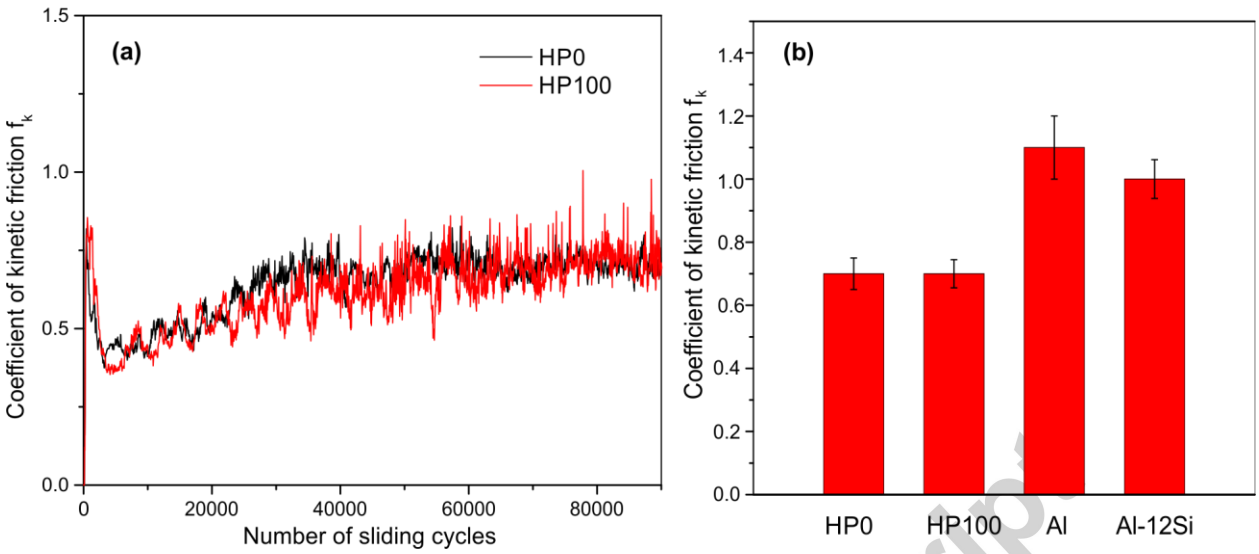

Fig. 2. (a) Kinetic friction coefficient between the investigated Al alloys and the martensitic chrome steel counter material as a function of the sliding cycles at half-amplitude of 1 mm for the $Al_{84}Ni_7Gd_6Co_3$ HP0 and HP100 alloys. (b) Comparison of the mean friction coefficient values between the counter-surfaces at the steady-state regime for the $Al_{84}Ni_7Gd_6Co_3$ and Al-12Si alloys, and pure Al.

Fig. 3a shows schematically the test configuration. Fig. 3b shows the wear scar on the surface of the HP100 specimen after a reciprocating sliding wear test with half-slip amplitude of 1 mm, and Fig 3c depicts a 3-D profile of the wear scar. Based on the surface profile of the wear track, the reciprocating sliding wear volume was calculated using the following equation [27, 33]:

$$V_f = h^2\left(3R_f - h\right)/3, \qquad (1)$$

where V_f is the volume loss, h is depth of the fretting scar, and R_f is given by the following formula:

$$R_f = (T^2 + h^2)/2h \quad , \qquad (2)$$

where T is calculated as $(d_1 \times d_2)^{-0.5} / 2$, with d_1 and d_2 being the principal diameters of the wear scar and any deviation from perfect circular shape was taken into account.

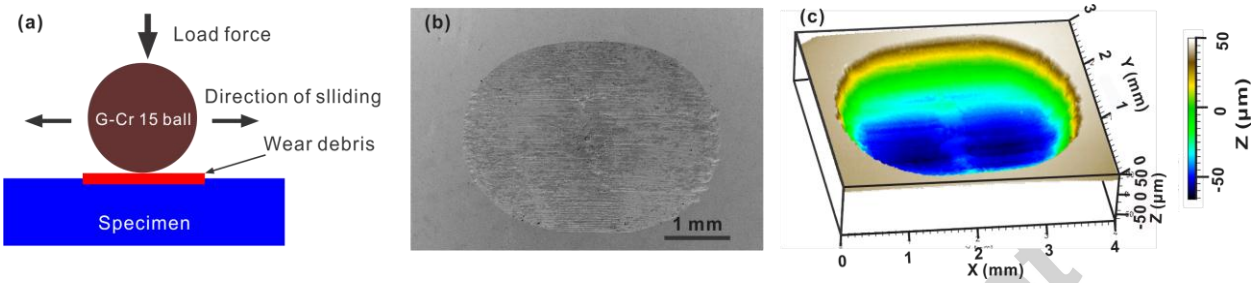

Fig. 3. Wear surface morphology: (a) test configuration, (b) SEM micrograph of HP100, (c) three-dimensional view of the wear scar.

Fig. 4 shows the volume loss for the nanocrystalline $Al_{84}Ni_7Gd_6Co_3$ alloys after the wear tests as a function of the half-sliding amplitude. The volume loss increases with increasing half-slip amplitude approximately proportional to the total sliding distance. The lower volume wear loss for the harder HP100 (4.3 GPa, lower than that for the softer HP0, 3.1 GPa), indicates enhanced wear performance of HP100 compared to HP0. For example, when the half amplitude is 1 mm, the volume loss is 0.12 and 0.14 mm^3 for HP100 and HP0, respectively.

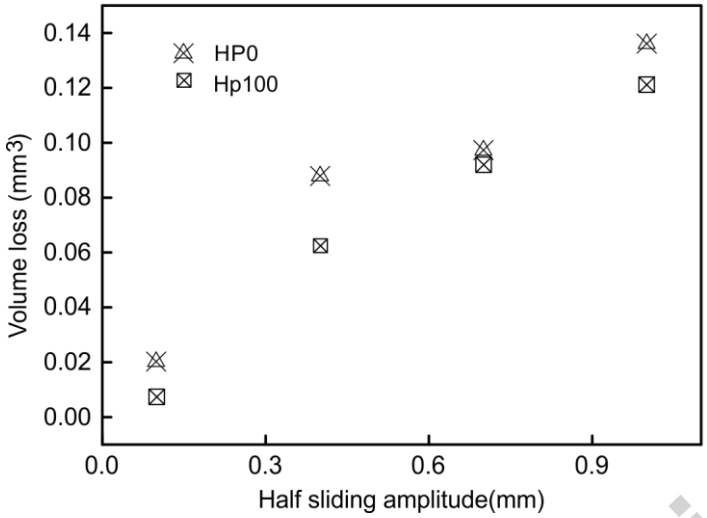

Fig. 4. Wear volume loss vs. half-amplitude for the HP0 and HP100 alloys.

Fig. 5 compares the volume loss for the $Al_{84}Ni_7Gd_6Co_3$ alloys with that for pure Al and Al-12Si after the wear tests with half-sliding amplitude of 1mm. It can be clearly seen that the wear volume for the nanocrystalline $Al_{84}Ni_7Gd_6Co_3$ alloys (HP0 and HP100) is much lower than that for pure Al and Al-12Si, indicating the significantly enhanced wear resistance of these alloys. The wear volumes presented in Fig 5, exhibit a clear qualitative correlation with the hardness of the investigated materials. The superior wear performance of the nanocrystalline $Al_{84}Ni_7Gd_6Co_3$ HP0 and HP100 alloys can be discussed in relation with the Archard's wear law [34]. The Archard's wear law, initially developed for sliding wear conditions, has been succesfully used to predict material loss in reciprocating sliding wear [35]:

$$V_s = \frac{kWL}{H} \tag{3}$$

where V_s is the volume loss, k is a dimensionless wear constant, W is the total normal load, L is the sliding distance and H is the hardness of the material. The hardness of HP100 alloys (4.3 GPa) is higher than that for HP0 (3.1 GPa), thus, as expected, the wear volume loss is lower for

HP100 than HP0. This trend follows a satisfactory correlation with eq. 3 within the margins of the experimental error. Comparing the nanocrystalline $Al_{84}Ni_7Gd_6Co_3$ HP0 and HP100 alloys with pure Al and Al-12Si, the higher hardness of the former results in the significantly higher wear resistance and lower volume loss as observed in Fig. 5. The relationship between the volume loss and hardness does not directly follow the Archard's equation if the wear constant k is considered the same for all the examined materials. However, the wear constant k is related to the nature and the chemistry of the counter-surfaces in relative motion and, therefore, different values of k are expected for the nanocrystlline $Al_{84}Ni_7Gd_6Co_3$, pure Al and Al-12Si.

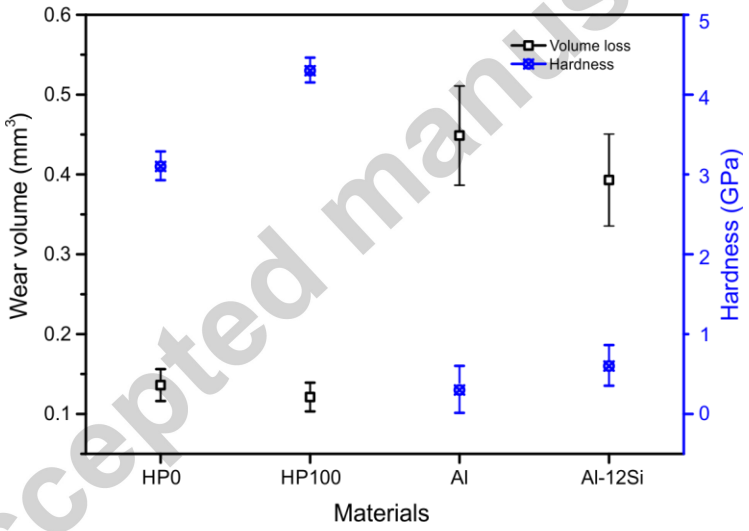

Fig. 5. Wear volume loss for the nanocrystalline $Al_{84}Ni_7Gd_6Co_3$ alloys (HP0 and HP100), pure Al and Al-12Si alloy after wear tests with half-sliding amplitude of 1 mm.

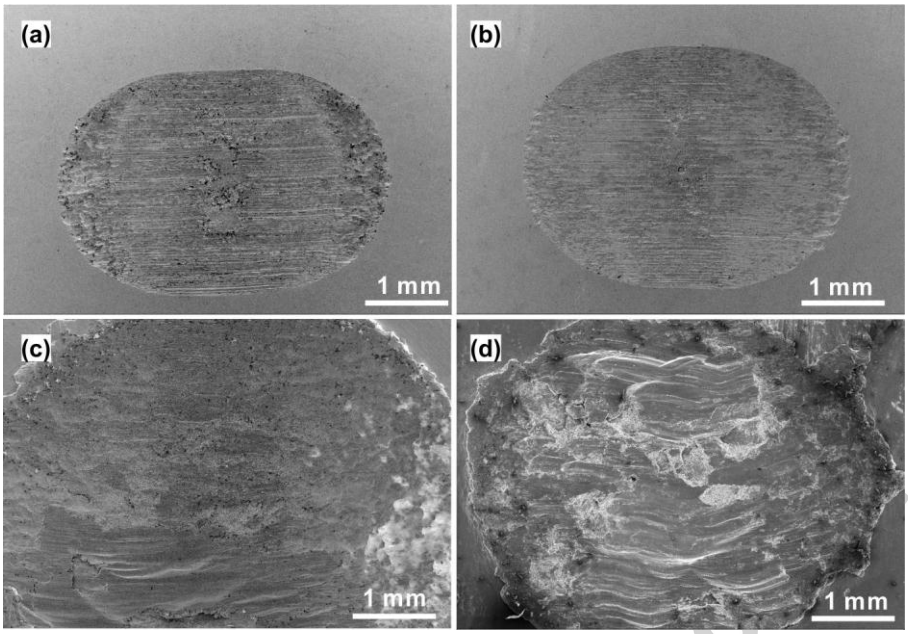

Fig. 6. SEM images of the wear surface morphologies of the samples: (a) HP0, (b) HP100, (c) pure Al, and (d) Al-12Si alloy.

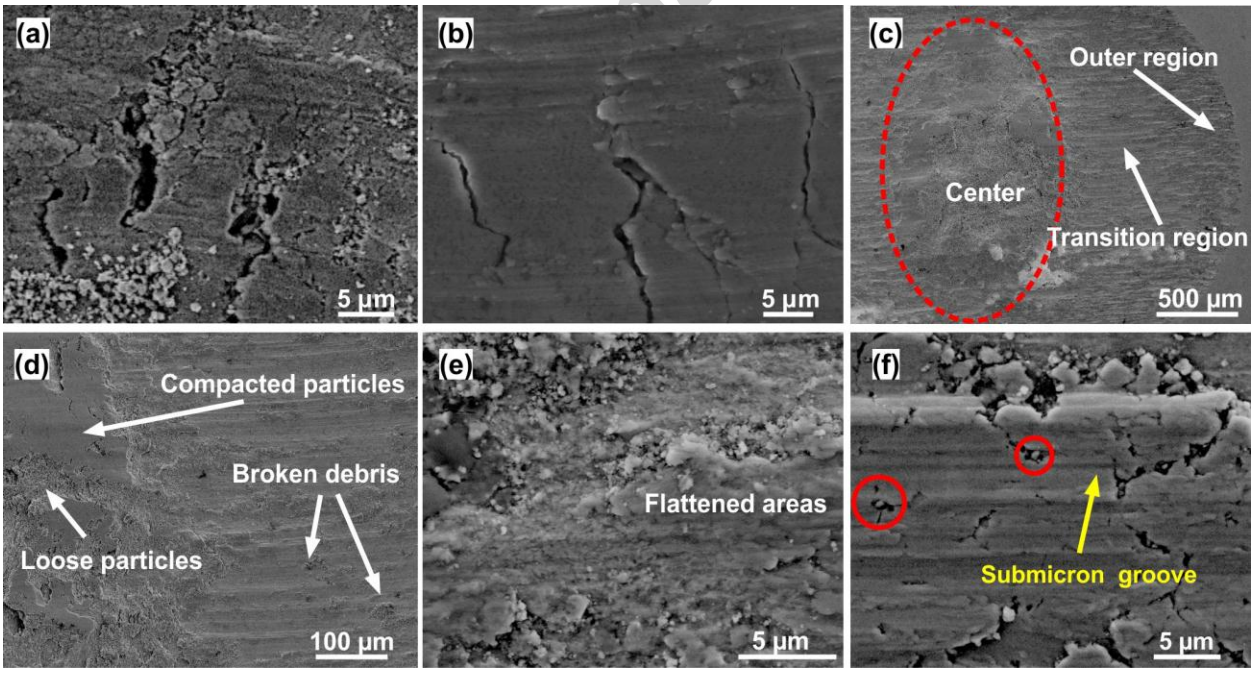

Fig. 7. SEM images of the wear surface morphologies: (a) pure Al, (b) Al-12Si alloy, (c-e) HP0, and (f) HP100.

It is interesting to examine the differences in the wear mechanisms between the hard nanocrystalline $Al_{84}Ni_7Gd_6Co_3$ alloys and the softer Al and Al-12Si. Fig. 6 shows the morphology of the wear scars after the wear tests. The wear scars on pure Al (Fig. 6c) and Al-12Si (Fig. 6d) have bigger size than those on the nanocrystalline $Al_{84}Ni_7Gd_6Co_3$ HP0 and HP100 alloys, in accordance with the results shown in Fig. 3 and Fig. 4. The wear scar morphology of Figs. 6c and 6d indicates plastic deformation and plowing action of the softer Al and Al-12Si surfaces from the harder steel counter-material. A closer look of the morphology after the fretting tests reveals the presence of metallic debris, oxide particles, scratches, craters and signs of plastic deformation in the wear scars of on Al and Al-12Si surfaces, Figs. 7a and 7b. In addition, many cracks were observed on the worn surfaces for both pure Al and Al-12Si, which may give rise to wear by delamination. Unlike pure Al and Al-12Si, the nanocrystalline $Al_{84}Ni_7Gd_6Co_3$ alloys exhibit three-body abrasion wear conditions resulting from their unique microstructure and the high volume fraction of nanometric intermetallic compounds and nanocrystalline Al matrix, as shown in Fig. 1. In the wear scars of the nanocrystalline $Al_{84}Ni_7Gd_6Co_3$ alloys two main features can be observed (Figs. 7c-7f): submicron grooves created by an abrasive wear mechanism and the accumulation and compaction of wear debris that acts as a protective layer for the extensive wear of the these alloys. The particulate debris results from the wear of the surface layers of the nanocrystalline Al alloys at the initial steps of the wear test probably as a result of fretting fatigue damage and the brittle fracture of the intermetallic phases. The formation of large amount of submicron hard debris leads to three-body abrasive conditions. A large part of the debris accumulates in the central region of the scars and becomes compacted and/or flattened during by the subsequent motion of the steel counter-face, Fig. 7c. The compaction of the loose debris particles in the central part of the scar can be

facilitated by a temperature rise during the sliding and wear process [33]. The rise of the temperature is often associated with the velocity of the relative motion and, therefore, it is expected to be higher in the center of the reciprocating sliding wear scar compared to the outer regions and for the wear tests with higher displacement amplitude (half amplitude: 1 mm). The sliding velocity under reciprocating sliding wear conditions can be estimated from the relation $V_s=4df$, where f is the frequency and d is the displacement [33]. On the other hand, the loose submicron debris particles lead to three third body abrasion conditions resulting in the formation of grooves and scratches in the wear track (Fig. 7f). Although the width of the grooves may vary depending on the size of the particulate debris, the vast majority of the grooves are smaller than 1 μm in width, in accordance with the size of the submicron particulate debris, Fig. 7f. The flattened areas can be delaminated more easily compared to the metal matrix; the red circles in Fig. 7f highlight the formation of cracks due to embedded submicron debris on the flattened areas. However, no cracks in the metal matrix are observed. In the outer regions of the wear scars, loose particulate debris can be found with less flattened and compacted areas than that in the center of the scar. This wear scenario is schematically depicted in Fig. 8; in the initial steps of the wear process, the surface layers of the nanocrystalline alloys are worn, probably due to fretting surface fatigue, producing particulate debris that creates a third body between the contact of the two counter-surfaces, Figs. 8a and 8b. The debris can be flattened and/or sintered under the subsequent action of the steel counter-face, Fig. 8c-8d, creating a body that protects the nanocrystalline alloys from extensive wear and thus contributing to their enhanced wear resistance. Thus, the compacted debris plays a beneficial role for protecting the fresh metal matrix from wear.

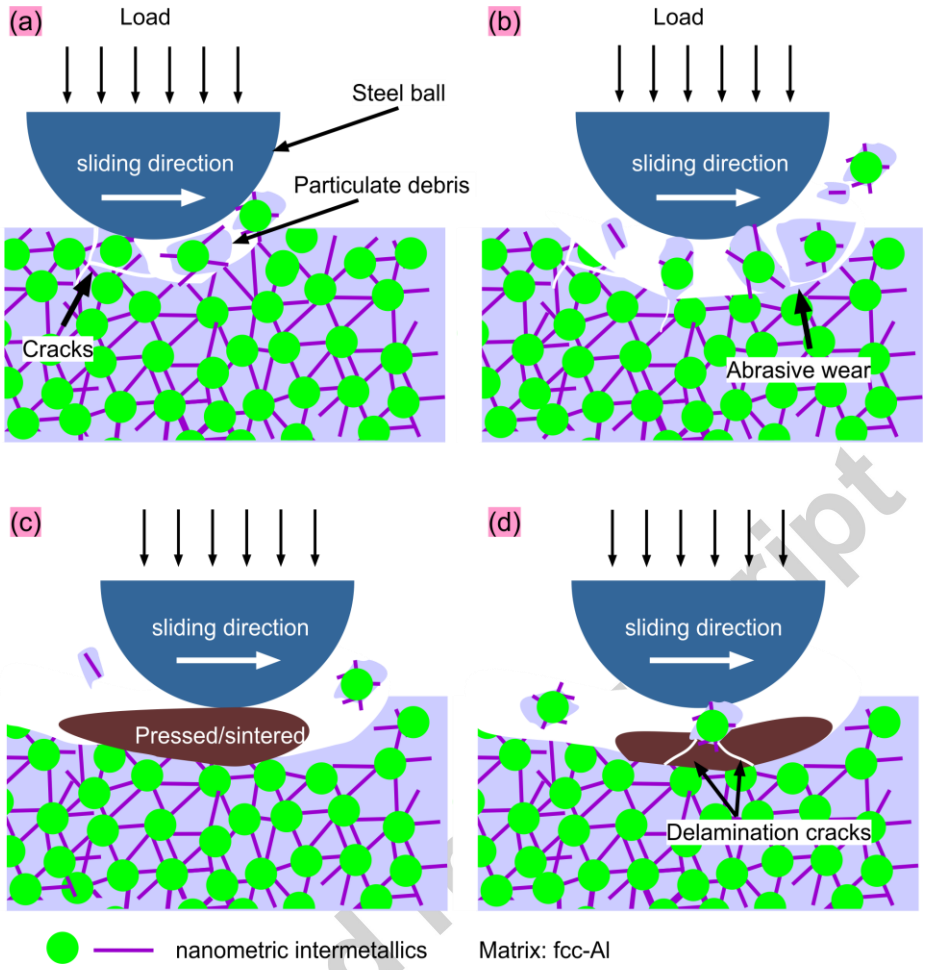

Fig. 8. Schematic illustration of the wear mechanisms in Al-Ni-Gd-Co nanocrystalline alloys.

Conclusions

In this work, the reciprocating sliding wear behavior of high-strength nanocrystalline $Al_{84}Ni_7Gd_6Co_3$ alloys produced from amorphous precursors has been studied under unidirectional small amplitude oscillatory motion conditions. The exceptionally high hardness of these alloys lead to significantly enhanced wear resistance compared to pure Al and Al-12Si alloys. The volume loss for the $Al_{84}Ni_7Gd_6Co_3$ nanocrystalline alloy was found to be 3 to 4 times lower than that for pure aluminum and Al-12Si alloy. The enhanced wear performance of $Al_{84}Ni_7Gd_6Co_3$ nanocrystalline alloy is related to the unique microstructure consisting of about

80 vol.% nanometric intermetallic compounds and 20 vol.% nanocrystalline Al, which leads to ultra-high hardness values between 3-4.5 GPa, values that are the highest ever reported for Al alloys. Under the small amplitude sliding motion of the counter-surfaces, particulate debris is created probably due to fretting surface fatigue of the nanocrystalline $Al_{84}Ni_7Gd_6Co_3$ nanocrystalline alloy during the initial stages of the wear tests leading to three body abrasive wear conditions. Under the subsequent motion of the steel counter-surface and the relative temperature rise, the debris can be flattened, compacted and sintered creating a body that protects the nanocrystalline alloys from extensive wear and thus contributing to the enhanced wear resistance.

Acknowledgements

Support from JSPS KAKENHI Grants: Number #15K18201, #16K18253, the World Premier International Research Center Initiative (WPI) of MEXT, Japan, Major Special Project for Science and Technology of Guangdong Province (No. 2015B090926004) and Guangdong Natural Science Foundation for Research Team (No. 2015A030312003) is gratefully acknowledged.

References:

[1] Kumar K, Van Swygenhoven H, Suresh S. Mechanical behavior of nanocrystalline metals and alloys. Acta Mater. 2003;51:5743–74.

[2] A. Inoue, Amorphous, nanoquasicrystalline and nanocrystalline alloys in Al-based systems, Prog. Mater. Sci. 43 (1998) 365–520.

[3] S. Scudino, K.B. Surreddi, H.V. Nguyen, G. Liu, T. Gemming, M. Sakaliyska, J.S. Kim, J. Vierke, M. Wollgarten, J. Eckert, High-strength $Al_{87}Ni_8La_5$ bulk alloy produced by spark plasma sintering of gas atomized powders, J. Mater. Res. 24 (2009) 2909–2916.

[4] Y. Kawamura, H. Mano, A. Inoue, Nanocrystalline aluminum bulk alloys with a high strength of 1420 MPa produced by the consolidation of amorphous powders, Scripta Mater. 44 (2001) 1599–1604.

[5] Z. Wang, R.T. Qu, S. Scudino, B.A. Sun, K.G. Prashanth, D.V. Louzguine-Luzgin, M.W. Chen, Z.F. Zhang, J. Eckert, Hybrid nanostructured aluminum alloy with super-high strength, NPG Asia Materials 7 (2015) e229.

[6] A. Inoue, H. Kimura, Fabrications and mechanical properties of bulk amorphous, nanocrystalline, nanoquasicrystalline alloys in aluminum-based system, J. light met. 1 (2001) 31–41.

[7] T. Sasaki, K. Hono, J. Vierke, M. Wollgarten, J. Banhart, Bulk nanocrystalline $Al_{85}Ni_{10}La_5$ alloy fabricated by spark plasma sintering of atomized amorphous powders, Mater. Sci. Eng. A 490 (2008) 343–350.

[8] D. Roy, R. Mitra, T. Chudoba, Z. Witczak, W. Lojkowski, H.-J. Fecht, I. Manna, Structure and mechanical properties of $Al_{65}Cu_{20}Ti_{15}$-based amorphous/nanocrystalline alloys prepared by high-pressure sintering, Mater. Sci. Eng. A 497 (2008) 93–100.

[9] A. Inoue, Y. Horio, Y. Kim, T. Masumoto, Elevated-temperature strength of an $Al_{88}Ni_9Ce_2Fe_1$ amorphous alloy containing nanoscale fcc-Al particles, Mater. Trans. JIM, 33 (1992) 669–674.

[10 Y. Li, K. Georgarakis, S. Pang, J. Antonowicz, F. Charlot, A. LeMoulec, T. Zhang, A.R. Yavari, AlNiY chill-zone alloys with good mechanical properties, J. Alloys Compd. 477 (2009) 346–349.

[11]Y. Li, K. Georgarakis, S. Pang, F. Charlot, A. LeMoulec, S. Brice-Profeta, T. Zhang, A.R. Yavari, Chill-zone aluminum alloys with GPa strength and good plasticity, J. Mater. Res. 24 (2009) 1513–1521.

[12] ASM Handbook, vol. 18: Friction, Lubrication, and Wear Technology, ASM International (1992)

[13] K. Nimura, T. Sugawara, T. Jibiki, S. Ito, M. Shima, Surface modification of aluminum alloy to improve fretting wear properties, Tribol. Int. 93, Part B (2016) 702–708.

[14] E. Rabinowicz, Friction and Wear of Materials, 2nd Edition, John Wiley and Sons, 1995

[15] D. Jeong, F. Gonzalez, G. Palumbo, K. Aust, U. Erb, The effect of grain size on the wear properties of electrodeposited nanocrystalline nickel coatings, Scripta Mater. 44 (2001) 493–499.

[16] C.N. Panagopoulos, K.G. Georgarakis, P.E. Agathocleous, Sliding wear behaviour of zinc-nickel alloy electrodeposits, Tribol. Int. 36 (2003) 619–623.

[17] C.N. Panagopoulos, K.G. Georgarakis, S. Petroutzakou, Sliding wear behaviour of zinc-cobalt alloy electrodeposits, J. Mater. Process. Technol. 160 (2005) 234–244.

[18] E.P. Georgiou, S. Achanta, S. Dosta, J. Fernandez, P. Matteazzi, J. Kusinski, R.R. Piticescu, and J.-P. Celis, Structural and Tribological Properties of Supersonic Sprayed Fe-Cu-Al-Al_2O_3 Nanostructured Cermets, Appl. Surf. Sci. 275 (2013) 142–147.

[19] X.Y. Li, K.N. Tandon, Microstructural characterization of mechanically mixed layer and wear debris in sliding wear of an Al alloy and an Al based composite, Wear 245 (2000) 148–161.

[20] Z.R. Zhou, S.R. Gu, L.Vincent, An investigation of the fretting wear of two aluminium alloys, Tribol. Int. 30 (1997) 1–7.

[21] I. Baker, Y. Sun, F.E. Kennedy, P.R. Munroe, Dry sliding wear of eutectic Al–Si, J. Mater. Sci. 45 (2009) 969.

[22] C. Schuh, T. Nieh, T. Yamasaki, Hall–Petch breakdown manifested in abrasive wear resistance of nanocrystalline nickel, Scripta Mater. 46 (2002) 735–740.

[23] C.N. Panagopoulos, K.G. Georgarakis, A. Anagnostopoulou, The influence of grain size on the sliding wear behaviour of zinc, Mater. Lett. 60 (2006) 133–136.

[24] T. Gloriant, A. Greer, Al-based nanocrystalline composites by rapid solidification of Al-Ni-Sm alloys, Nanostruct Mater. 10 (1998) 389–396.

[25] M. Chen, T. Perry, A.T. Alpas, Ultra-mild wear in eutectic Al–Si alloys, Wear 263 (2007) 552–561.

[26] K.G. Basavakumar, P.G. Mukunda, M. Chakraborty, Dry sliding wear behaviour of Al–12Si and Al–12Si–3Cu cast alloys, Mater. Design 30 (2009) 1258–1267.

[27] K. Prashanth, B. Debalina, Z. Wang, P. Gostin, A. Gebert, M. Calin, U. Kühn, M. Kamaraj, S. Scudino, J. Eckert, Tribological and corrosion properties of Al–12Si produced by selective laser melting, J. Mater. Res. 29 (2014) 2044–2054.

[28] Z. Wang, K.G. Prashanth, A.K. Chaubey, L. Löber, F.P. Schimansky, F. Pyczak, W.W. Zhang, S. Scudino, J. Eckert, Tensile properties of Al–12Si matrix composites reinforced with Ti–Al-based particles, J. Alloy Compd. 630 (2015) 256–259.

[29] H. Goto, K. Uchijo, Fretting wear of Al–Si alloy matrix composites, Wear 256 (2004) 630–638.

[30]J.D. Lemm, A.R. Warmuth, S.R. Pearson, P.H. Shipway, The influence of surface hardness on the fretting wear of steel pairs-Its role in debris retention in the contact, Tribol. Int. 81 (2014) 258–266.

[31] T. Kayaba, A. Iwabuchi, Effect of the hardness of hardened steels and the action of oxides on fretting wear, Wear 66 (1981) 27–41.

[32] A.J.W. Moore, W.J. McG. Tegart, Relation between Friction and Hardness, Proceedings of the Royal Society of London. Series A, Mathematical and Physical Sciences, Volume 212, Issue 1111, 1952, pp. 452–458.

[33] K. Elleuch, S. Fouvry, Wear analysis of A357 aluminium alloy under fretting, Wear 253 (2002) 662–672.

[34] J. Archard, Contact and rubbing of flat surfaces, J. Appl. Phys. 24 (1953) 981–988.

[35] I.R. McColl, J. Ding, S.B. Leen. Finite element simulation and experimental validation of fretting wear, Wear 256 (2004)1114–1127.

Highlights

- The reciprocating sliding wear behavior of high-strength nanocrystalline Al-based alloys has been studied.
- The nanocrystalline Al alloys exhibit excellent wear resistance being significantly smaller than those for pure Al and Al-12Si alloys.
- The enhanced wear resistance of the novel nanocrystaline Al alloys is related to their ultra-high hardness and the hybrid nanostructure.
- The lower friction coefficient is mainly attributed to the formation of surface oxide layers as well as the formation of a tribo-layer of debris between the contact surfaces.

2017-04-23

Reciprocating sliding wear behavior of high-strength nanocrystalline Al84Ni7Gd6Co3 alloys

Wang, Z.

Elsevier

Wang Z, Georgarakis K, Zhang WW, Prashanth KG, Eckert J, Scudino S, Reciprocating sliding þÿwear behavior of high-strength nanocrystalline Al84Ni7Gd6Co3 alloys, W July 2017, pp. 78-84

http://dx.doi.org/10.1016/j.wear.2017.04.013